

CHEMOTACTICALLY INDUCED SEARCH AND DEFENSE STRATEGIES IN A TRITROPHIC SYSTEM

NESTOR ANAYA*

Departamento de Matemáticas
Facultad de Ciencias
Ciudad Universitaria, CDMX 04510 México

MANUEL FALCONI AND GUILMER GONZÁLEZ

Departamento de Matemáticas
Facultad de Ciencias
Ciudad Universitaria, CDMX 04510 México

(Communicated by the associate editor name)

ABSTRACT. In this paper we study the question of the survival of a predator which in a static scenario vanishes. we analyze the role of migration on the coexistence of three species interacting through a intraguild relationship.

1. Introduction. Individual movement regulated by concentrations of chemical substances is a very frequent natural phenomenon; known as *Chemotaxis* is an important mechanism, for instance, of bacterial populations in search of nutrients or to establish symbiotic relationships (see [24]). Chemical components has been observed as a defense strategy of several species. To get some insight about this process, in [20] were studied the chemical defense of two species of brown alga *Dictyota menstrualis* and *Dictyota mertensii* used against the limited mobility herbivores, the amphipod *Parhyale hawaiiensis* and the crab *Pachygrapsus transversus*. In fact, natural defense against predation is very well documented and it is present in both invertebrate and vertebrate species, see [7], [9], [10], [26],[3]. On the other hand, the study about the relationship of organism dispersal and community structure of interacting species has a long history. Since the works of Kolmogorov [15] and Skellam [22], mathematical modeling of diffusion and random walk has been widely applied in the study of the effect of individual movement on the dynamic properties of different kinds of species interaction. Among the recent works on this topic it is [28] where the authors consider a tritrophic food chain with predators and one resource; the existence and boundedness of solutions and stability of equilibrium solutions are analyzed. Stability and Turing patterns of a diffusive predator-prey model have been analyzed in [23]. Diffusion and delay effect has been incorporated in an intraguild predation model in [11], where the authors studied how the delay on the conversion rate of mesopredator induces spatiotemporal patterns. About

2020 *Mathematics Subject Classification.* 35K57, 35Q92, 92D25.

Key words and phrases. Competing species, Intraguild predation model, Chemotaxis, Active-search hunting,

The first author is supported by NSF grant xx-xxxx.

*Corresponding author: Nestor Anaya.

diffusion in predator-prey context see [27], [1]. In this work we analyzed how the emission of chemical substances which attract predators of consumers of a resource impact the spatial distribution of species. A laboratory study on this topic is [14] where Kessler and Baldwin have found that volatile emissions from *Nicotiana attenuata* could reduce the number of herbivores up to 90%.

In this work, we consider an intraguild predation model of one resource and two predators; the importance of this interaction for population ecology has been explained by Polis and Holt in [31]. We consider that meso predator feed on a resource which grows according to a logistic growth law and it is consumed by a top predator; functional responses of meso and top predators are of Holling II type. Predators and preys diffuse in a connected bounded region $\Omega \subset \mathbb{R}^2$ of the plane. We consider two cases: in the first case, the model is

$$\begin{aligned} \frac{\partial u}{\partial t} &= d_0 \Delta u + \alpha u \left(1 - \frac{u}{K}\right) - \frac{buv}{u+a}, \\ \frac{\partial v}{\partial t} &= d_1 \Delta v + \gamma \frac{buv}{u+a} - \frac{cvw}{v+d} - \mu v, \\ \frac{\partial w}{\partial t} &= d_2 \Delta w + \beta \frac{cvw}{v+d} - \nu w - \nabla \cdot (\chi_1(v, w) \nabla v), \end{aligned} \quad (1)$$

the random dispersal of top predators is tempered by a certain tendency to move up the gradient of meso predators.

In the second case, as a chemotactic defense mechanism of the prey is considered, the resource population attracts top predators which feeds on mesopredator; this kind of indirect defense against predators has been reported in [2], see also [3]; 2) top predator in search of food moves towards areas where the mesopredator population is increasing. The model is given by

$$\begin{aligned} \frac{\partial u}{\partial t} &= d_0 \Delta u + \alpha u \left(1 - \frac{u}{K}\right) - \frac{buv}{u+a}, \\ \frac{\partial v}{\partial t} &= d_1 \Delta v + \gamma \frac{buv}{u+a} - \frac{cvw}{v+d} - \mu v, \\ \frac{\partial w}{\partial t} &= d_2 \Delta w + \beta \frac{cvw}{v+d} - \nu w - \nabla \cdot (\chi_2(u, w) \nabla u), \end{aligned} \quad (2)$$

in this model the random movement is regulated by the gradient of population density of the resource. The carrying capacity $K = K(x, y)$ is non-negative function defined in Ω and describes the different suitability of the niches for the resource species. Niche suitability and size population has been addressed in [16]. It is assumed that the flux vanishes in the boundary of Ω ,

$$\frac{\partial u}{\partial \eta}(x, t) = \frac{\partial v}{\partial \eta}(x, t) = \frac{\partial w}{\partial \eta}(x, t) = 0, x \in \partial\Omega, t > 0 \quad (3)$$

where $\partial/\partial\eta = \eta \cdot \nabla$, and η is the normal vector to $\partial\Omega$.

The carrying capacity is denoted by K , α is the intrinsic growth of the resource u ; b y c are the mortality rate by predation of u and v , respectively. The conversion rate of biomass captured by v and w are γ and β , respectively. In Model 1 it is assumed that the regulating mechanism against of random dispersal of w depends on a volatile substance is generated by u ; in Model 2 is generated by v . Two predators which feed on a common resource subject to a Lotka-Volterra interaction was considered in [34]; diffusive movement of predators is controlled by the prey density gradient. In [25] was analyzed a predator-prey model where predator moves

toward the gradient of a chemical released by prey.

The underlying ordinary differential system corresponding to models 2 and 1 is given by

$$\begin{aligned} u' &= \alpha u \left(1 - \frac{u}{K}\right) - \frac{buv}{u+a}, \\ v' &= \gamma \frac{buv}{u+a} - \frac{cvw}{v+d} - \mu v, \\ w' &= \beta \frac{cvw}{v+d} - \nu w. \end{aligned} \tag{4}$$

The system (4) has the following equilibrium points

- i) $P_1(0, 0, 0)$
- ii) $P_2(K, 0, 0)$
- iii) $P_3\left(\frac{a\mu}{b\gamma-\mu}, \frac{a\alpha\gamma(b\gamma K - \mu(a+K))}{K(b\gamma-\mu)^2}, 0\right)$.

Under appropriate conditions, this system posses two equilibrium points $P_4(u_1, v_1, w_1)$ and $P_5(u_2, v_2, w_2)$ with positive coordinates given by

$$\begin{aligned} u_1 &= \frac{1}{2} \left(-a + K - \sqrt{\frac{c\alpha\beta(a+K)^2 - (4bdK + (a+K)^2\alpha)\nu}{(c\beta - \nu)\alpha}} \right) \\ v_1 &= \frac{d\nu}{c\beta - \nu} \\ w_1 &= \frac{(d+v_1)(b\gamma u_1 - (a+u_1)v_1\mu)}{c(a+u_1)} \\ u_2 &= \frac{1}{2} \left(-a + K + \sqrt{\frac{c\alpha\beta(a+K)^2 - (4bdK + (a+K)^2\alpha)\nu}{(c\beta - \nu)\alpha}} \right) \\ v_2 &= \frac{d\nu}{c\beta - \nu} \\ w_2 &= \frac{(d+v_2)(b\gamma u_2 - (a+u_2)v_2\mu)}{c(a+u_2)}. \end{aligned}$$

The local dynamics around the equilibrium points of this system is depicted in Appendix A.

2. Existence of positive solution. In this section we provide conditions for the existence of positive solutions of systems 1 and 2 for the initial conditions

$$t = 0: u = u_0(x), v = v_0(x), w = w_0(x), x \in \Omega \tag{5}$$

and the boundary conditions given by (3). Let $p > n \geq 1$; then $W^{1,p}(\Omega, \mathbb{R}^n)$ is continuously embedded in the continuous function space $C(\Omega; \mathbb{R}^n)$. Let

$$X := \{y \in W^{1,p}(\Omega, \mathbb{R}^3) \mid \eta \cdot \nabla y|_{\partial\Omega} = 0\}.$$

Theorem 2.1. *If $(u_0, v_0, w_0) \in X$, then*

- *There exists $T = T_{\max} \in [0, \infty)$, which depends on the initial conditions (5) such that the problem (1),(3)-(5) has a unique maximal solution (u, v, w)*

on $\Omega \times [0, T_{\max})$ and $(u(\cdot, t), v(\cdot, t), w(\cdot, t)) \in C((0, T_{\max}), \Omega)$, $(u, v, w) \in C^{2,1}((0, T_{\max}) \times \overline{\Omega}, \mathbb{R}^3)$;

- If $u_0, v_0, w_0 \geq 0$ on $\overline{\Omega}$, then $u, v, w \geq 0$ on $\Omega \times [0, T_{\max})$;
- If $\|(u, w, w)(\cdot, t)\|_{L^\infty(\Omega)}$ is bounded for all $t \in [0, T_{\max})$, then $T_{\max} = +\infty$; equivalently, (u, v, w) is a global solution.

Proof. Let $z = (u, v, w)^3$. Then, (1), (3) and (5) can be written as

$$\begin{aligned} z_t &= \nabla \cdot (A(z) \nabla z) + F(z) \text{ on } \Omega \times [0, \infty) \\ B_z &= \frac{\partial}{\partial \nu} z = 0 \text{ on } \partial\Omega \times [0, \infty) \\ z(\cdot, 0) &= (u_0, v_0, w_0) \text{ en } \Omega, \end{aligned} \quad (6)$$

where

$$A[z] = \begin{bmatrix} d_0 & 0 & 0 \\ 0 & d_1 & 0 \\ 0 & -\chi_1 & d_2 \end{bmatrix}$$

and

$$F(z) = \begin{bmatrix} u \left(\alpha \left(1 - \frac{u}{K} \right) - \frac{bv}{u+a} \right) \\ v \left(\gamma \frac{bu}{u+a} - \frac{cw}{v+d} - \mu \right) \\ w \left(\beta \frac{cv}{v+d} - \nu \right) \end{bmatrix}$$

The result follows from [12]. \square

According to the above theorem, to prove the existence of global solutions it is necessary to show that u, v and w are uniformly bounded in $L^\infty(\Omega)$.

Theorem 2.2. *If $(u_0, v_0, w_0) \in X$, then the solutions of the system (1), (3) and (5) are bounded.*

Proof. Let $W(x, t) = u + \frac{1}{\gamma}v + \frac{1}{\gamma\beta}w$, so

$$\begin{aligned} \frac{d}{dt} \int_{\Omega} (W(x, t)) &= \int_{\Omega} \left(d_0 \Delta u + \alpha u \left(1 - \frac{u}{K} \right) - \frac{buv}{u+a} \right) dx + \int_{\Omega} \left(\frac{1}{\gamma} \left(d_1 \Delta v + \gamma \frac{buv}{u+a} - \frac{cvw}{v+d} - \mu v \right) \right) dx \\ &\quad + \int_{\Omega} \left(\frac{1}{\gamma\beta} \left(d_2 \Delta w + \beta \frac{cvw}{v+d} - vw - \nabla \cdot (\chi_1(v, w) \nabla v) \right) \right) dx \\ &= \int_{\Omega} \left(d_0 \Delta u + \frac{1}{\gamma} d_1 \Delta v + \frac{1}{\gamma\beta} d_2 \Delta w \right) dx \\ &\quad + \int_{\Omega} \left(\alpha u \left(1 - \frac{u}{K} \right) - \frac{buv}{u+a} + \frac{buv}{u+a} - \frac{c}{\gamma} \frac{vw}{v+d} - \frac{\mu}{\gamma} v + \frac{c}{\gamma} \frac{cvw}{v+d} - \frac{\nu}{\gamma\beta} w \right) dx \\ &\leq \int_{\Omega} \left(\alpha u \left(1 - \frac{u}{K} \right) - \frac{\mu}{\gamma} v - \frac{\nu}{\gamma\beta} w \right) dx \end{aligned}$$

It follows that

$$\frac{d}{dt} \int_{\Omega} W dx + \int_{\Omega} \left(\frac{\mu}{\gamma} v + \frac{\nu}{\gamma\beta} w \right) dx \leq \int_{\Omega} \alpha u \left(1 - \frac{u}{K} \right) dx. \quad (7)$$

On the other hand, let $\mu_0 = \min\{\mu, \nu\}$ that implies

$$\frac{d}{dt} \int_{\Omega} W dx + \mu_0 \int_{\Omega} \left(\frac{1}{\gamma} v + \frac{1}{\gamma\beta} w \right) dx \leq \frac{d}{dt} \int_{\Omega} W dx + \int_{\Omega} \left(\frac{\mu}{\gamma} v + \frac{\nu}{\gamma\beta} w \right) dx. \quad (8)$$

From (7) and (8), we obtain that

$$\frac{d}{dt} \int_{\Omega} W dx + \mu_0 \int_{\Omega} \left(u + \frac{1}{\gamma} v + \frac{1}{\gamma\beta} w \right) dx \leq \int_{\Omega} \left(\alpha u \left(1 - \frac{u}{K} \right) + \mu_0 u \right) dx \quad (9)$$

Note that

$$\begin{aligned} \int_{\Omega} \left((\alpha + \mu_0) u - \frac{\alpha u^2}{K} \right) dx &\leq \int_{\Omega} \frac{1}{4} \frac{K (\alpha + \mu_0)^2}{\alpha} dx \\ &= \frac{1}{4} \frac{K (\alpha + \mu_0)^2}{\alpha} |\Omega| \end{aligned} \quad (10)$$

Now, let $K_0 = \frac{1}{4} \frac{K (\alpha + \mu_0)^2}{\alpha} |\Omega|$, then from (9) and (10) we have that

$$\frac{d}{dt} \int_{\Omega} W dx + \mu_0 \int_{\Omega} \left(u + \frac{1}{\gamma} v + \frac{1}{\gamma\beta} w \right) dx \leq K_0$$

from this, is clearly evident that

$$\int_{\Omega} \left(u + \frac{1}{\gamma} v + \frac{1}{\gamma\beta} w \right) dx \leq K_0 + ce^{-t}$$

It follows that solutions are bounded, since u, v, w are nonnegative. \square

The proof of the following theorem is similar to those of Theorem 2.1.

Theorem 2.3. *Let $(u_0, v_0, w_0) \in X$.*

- *There exists $T = T_{\max} \in [0, \infty)$, which depends on the initial conditions (5) such that the problem (2), (3) and (5) has a unique maximal solution (u, v, w) on $\Omega \times [0, T_{\max})$ and $(u(\cdot, t), v(\cdot, t), w(\cdot, t)) \in C((0, T_{\max}), \Omega)$, $(u, v, w) \in C^{2,1}((0, T_{\max}) \times \overline{\Omega}, \mathbb{R}^3)$;*
- *If $u_0, v_0, w_0 \geq 0$ on $\overline{\Omega}$, then $u, v, w \geq 0$ on $\Omega \times [0, T_{\max})$;*
- *If $\|(u, w, w)(\cdot, t)\|_{L^\infty(\Omega)}$ is bounded for all $t \in [0, T_{\max})$, then $T_{\max} = +\infty$; i.e., (u, v, w) is a globally bounded solution.*

Note that v and w vanish if $\gamma b \leq \mu$ and $\beta c \leq \nu$, respectively. From now on, we assume that $\gamma b > \mu$ and $\beta c > \nu$.

Let $Y = \left\{ U = (u, v, w) \in [C^1(\overline{\Omega})]^3 \mid \partial_\nu u(x) = 0, x \in \partial\Omega \right\}$, and let $\{\phi_{i,j}, j = 1, 2, \dots, \dim(E(\mu_i))\}$ be an orthonormal basis of $E(\mu_i)$ and $Y_{ij} = \{C \cdot \phi_{ij} \mid C \in \mathbb{R}^3\}$. Then, $Y_i = \bigoplus_{j=1}^{\dim(E(\mu_i))} Y_{ij}$, $Y = \bigoplus_{i=1}^{\infty} Y_i$.

Theorem 2.4. *If $bK\gamma - a\mu - K\mu < 0$ then the equilibrium point P_2 of system 1 is locally stable.*

Proof. Let $A[z] = \begin{pmatrix} d_0 & 0 & 0 \\ 0 & d_1 & 0 \\ 0 & -\chi_1 & d_2 \end{pmatrix}$ as in theorem 2.1 and $L = A[z] \Delta + J_1$ where J_1 is the Jacobian matrix of the system without diffusion evaluated at P_2 ; i.e.

$$J_1 = \begin{pmatrix} -\alpha & -\frac{bK}{a+K} & 0 \\ 0 & \frac{bK\gamma}{a+K} - \mu & 0 \\ 0 & 0 & -\nu \end{pmatrix}.$$

The linearization of the system at P_2 is $U_t = LU$. Y_i is invariant with respect to operator L for all $i \geq 1$; λ is an eigenvalue of L restricted to Y_i if and only if is an eigenvalue of matrix $-\mu_i A[z] \Delta + J_1$.

The characteristic polynomial of $\mu_i A [z] \Delta + J_1$ is

$$\varphi_i(\lambda) = (\lambda + \mu_i d_1 + \alpha) \left(\lambda + \mu_i d_2 - \frac{bK\gamma}{a+K} + \mu \right) (\lambda + \mu_i d_2 + \nu)$$

whose roots are $\varphi_i(\lambda) - \mu_i d_1 - \alpha$, $-\mu_i d_2 + \frac{bK\gamma}{a+K} - \mu$ and $-\mu_i d_2 - \nu$. Therefore, the point-spectrum of L consists of eigenvalues that satisfy $\{\operatorname{Re} \lambda \leq -(1/2) \max\{\alpha, -\frac{bK\gamma}{a+K} + \mu, \nu\}\}$ whenever $bK\gamma - a\mu - K\mu < 0$; from which stability around P_2 follows, [[5], Th. 5.1.1]. \square

The following section describes the spatial discretization that we apply to perform some numerical simulations of the previous models.

3. Spatial discretization.

3.1. Variational formulation. We consider a general reaction-diffusion problem with Neumann boundary conditions

$$-\Delta u + \mu u = f \quad \text{en } \Omega \quad (11)$$

$$u(x, 0) = u_0(x) \quad \text{en } \Omega \quad (12)$$

$$\partial_n u(x, t) = 0 \quad \text{en } \partial\Omega \quad (13)$$

where function $f \in C^0(\Omega)$ is regular, $\mu \in \mathbb{R}$. As it is usual $\partial_n u = \nabla u \cdot \mathbf{n}$, where \mathbf{n} is the exterior normal vector to $\partial\Omega$.

A classic solution of the above problem (11)–(13) is a function $u : \bar{\Omega} \mapsto \mathbb{R}$, $u \in C^2(\bar{\Omega})$ which satisfies (11)–(13). In order to facilitate the search of u we reformulate the problem to find a equivalent solution.

Let $v \in X := C^2(\bar{\Omega})$. Multiplying (11) by v it is obtained

$$-v\Delta u + \mu uv = fv$$

Integrating on Ω

$$-\int_{\Omega} v\Delta u \, d\Omega + \mu \int_{\Omega} uv \, d\Omega = \int_{\Omega} fv \, d\Omega \quad (14)$$

Applying the Green Theorem

$$\int_{\Omega} \nabla u \cdot \nabla v \, d\Omega - \int_{\partial\Omega} (\nabla u \cdot \mathbf{n})v \, dS + \mu \int_{\Omega} uv \, d\Omega = \int_{\Omega} fv \, d\Omega. \quad (15)$$

Since $\partial_n u = 0$ for $x \in \partial\Omega$, we have

$$\int_{\Omega} \nabla u \cdot \nabla v \, d\Omega + \mu \int_{\Omega} uv \, d\Omega = \int_{\Omega} fv \, d\Omega. \quad (16)$$

This expression is known as variational formulation of the problem (11)–(13), see [32]. Notice that in (16) it is only required that $u, v \in C^1(\bar{\Omega})$. Furthermore, they can even be just continuous.

3.2. Discretization Finite Element Method. Let $H^k(\Omega)$ a Sobolev space and $C^1(0, T, X)$ is the space of continuously differentiable functions from $[0, T]$ on X . Ω_h is a polygonal approximation of Ω . We consider a mesh T_h of Ω_h consisting of convex elements $E_i \in T_h$, $i \in I$, $I \subset \mathbb{N}$.

Let $\{\varphi_j(x, y)\}_{1 \leq j \leq N}$ be a base of V_h

$$\begin{aligned} u_h(x, y, t) &= \sum_{j=1}^N u_j(t) \varphi_j(x, y) \\ v_h(x, y, t) &= \sum_{j=1}^N v_j(t) \varphi_j(x, y) \\ w_h(x, y, t) &= \sum_{j=1}^N w_j(t) \varphi_j(x, y) \end{aligned}$$

$x, y \in \Omega$, $0 \leq t \leq T$. The basis $\varphi_j(x, y)$ are compact support functions and we use the usual linear elements $P1$ defined on triangles.

Parameter h represents the size of element E_i of mesh T_h and is defined as

$$h = \max_{E_i \in T_h} \text{diam}(E_i),$$

as $h \mapsto 0$, space V_h is closer to $H^k(\Omega)$.

4. Semi-discretization of time. Let

$$0 = t_0 < t_1 < \dots < t_N = T,$$

a partition of the interval $[0, T]$ with constant step $dt = t_{m+1} - t_m$ for all $m \in \{0, \dots, N-1\}$. The derivative with respect to time is approximated using forward finite differences

$$u_t = \frac{u^{m+1} - u^m}{dt}, \quad v_t = \frac{v^{m+1} - v^m}{dt}, \quad w_t = \frac{w^{m+1} - w^m}{dt}$$

where $u^m = u(x, t_m)$, $v^m = v(x, t_m)$, $w^m = w(x, t_m)$.

By substituting the above approximation in model (1) we obtain that

$$\begin{aligned} u^{m+1} &= u^m + dt \cdot d_0 \Delta u^{m+1} + dt \cdot \alpha u^{m+1} \left(1 - \frac{u^{m+1}}{K(x, y)}\right) - dt \cdot \frac{bu^{m+1}v^{m+1}}{u^{m+1} + a}, \\ v^{m+1} &= v^m + dt \cdot d_1 \Delta v^{m+1} + dt \cdot \gamma \frac{bu^{m+1}v^{m+1}}{u^{m+1} + a} - dt \cdot \frac{cv^{m+1}w^{m+1}}{v^{m+1} + d} - \mu v^m \quad (17) \\ w^{m+1} &= w^m + dt \cdot d_2 \Delta w^{m+1} + dt \cdot \beta \frac{cv^{m+1}w^{m+1}}{v^{m+1} + d} \\ &\quad - dt \cdot \nu w^{m+1} - dt \cdot \nabla \cdot (\chi_2(v^{m+1}, w^{m+1}) \nabla v^{m+1}). \end{aligned}$$

This is the Implicit Euler Method which depends on both $(x, y) \in \Omega$ for each element E_i and the boundary conditions

$$\nabla u^{m+1} \cdot \mathbf{n} = 0, \quad \nabla v^{m+1} \cdot \mathbf{n} = 0, \quad \nabla w^{m+1} \cdot \mathbf{n} = 0, \quad m \geq 0. \quad (18)$$

From the initial values u_0, v_0 , and w_0 , we compute the next iterations $(u_1, v_1, w_1), \dots, (u_N, v_N, w_N)$. The system (17) is solved by FEM, assuming that $u_0, v_0, w_0 \in C^2(\bar{\Omega})$, see [30]. To avoid some complications which arise from the nonlinearity involved in (17), the

terms corresponding to temporal variation are solved using a semi-implicit Runge-Kutta method of second order. The two steps of this computational process are depicted in the following. First, the right side of equations (1) are rewritten as

$$\begin{aligned} F(u, v, w) &= d_0 \Delta u + \alpha u \left(1 - \frac{u}{K(x, y)}\right) - \frac{buv}{u + a}, \\ G(u, v, w) &= d_1 \Delta v + \gamma \frac{buv}{u + a} - \frac{cvw}{v + d} - \mu v, \\ H(u, v, w) &= d_2 \Delta w + \beta \frac{cvw}{v + d} - \nu w - \nabla \cdot (\chi_2(v, w) \nabla v). \end{aligned} \quad (19)$$

The first step of the RK-method of second order consists in an one Euler step computed at central point of each time interval.

$$u^{m+1/2} = u^m + \frac{dt}{2} \cdot F(u^m, v^m, w^m) \quad (20)$$

$$v^{m+1/2} = v^m + \frac{dt}{2} \cdot G(u^m, v^m, w^m) \quad (21)$$

$$w^{m+1/2} = w^m + \frac{dt}{2} \cdot H(u^m, v^m, w^m) \quad (22)$$

In the second step, computations are made at time $m + 1$ like

$$u^{m+1} = u^m + dt \cdot F(u^{m+1/2}, v^{m+1/2}, w^{m+1/2}) \quad (23)$$

$$v^{m+1} = v^m + dt \cdot G(u^{m+1/2}, v^{m+1/2}, w^{m+1/2}) \quad (24)$$

$$w^{m+1} = w^m + dt \cdot H(u^{m+1/2}, v^{m+1/2}, w^{m+1/2}) \quad (25)$$

Now we considered the diffusion in an implicit form, then the schema becomes a semi-implicit one. For each step, the equations are solved by applying the FEM Galerkin-Ritz method described above.

5. Numerical simulations. In this section, some numerical simulations are carried out in order to obtain some knowledge about the effect on the population density of the indirect defense mechanism of the resource against the meso-predator, which consists on the attraction of the main predator towards the resource. This will be contrasted with the results of the corresponding simulations of model 1, in which the random diffusion of the main predator is regulated by a tendency to move towards the gradient of the meso-predator; this is the case of predators actively searching for prey, see [4], [6] and the references cited there. In all this section, we assume that $\alpha = 5$, $a = 2.0$, $b = 5$, $c = .01$, $d = 2.0$, $\beta = 1.0$, $\gamma = 1$, $\mu = .05$, $\nu = .05$. For this parameter values, the equilibrium points of system (4) are $P_0 = (0, 0, 0)$, $P_1 = (K, 0, 0)$, $P_2 = (\frac{2}{99}, \frac{200(99K-2)}{9801K}, 0)$, $P_3 = (k-2, 2, \frac{2(99K-200)}{K})$. Existence and stability properties of these equilibrium points are described in Table 1. For the numerical computations we assume that $\Omega = [-1, 1] \times [-1, 1]$ and we have used the FreeFem++ software [13].

5.1. Model 1: active-search hunting. In the following we consider Model (1) where the top predator is an active-search hunter. We take

$$\chi_1(v, w) = e_1 w - e_2 v.$$

TABLE 1.

Point	Existence Interval	Stable	Unstable
P_0	$K > 0$		$K > 0$
P_1	$K > 0$	$K < \frac{2}{99}$	$K > \frac{2}{99}$
P_2	$K > \frac{2}{99}$	$\frac{2}{99} < K < \frac{200}{99}$	$K > \frac{200}{99}$
P_3	$K > \frac{200}{99}$	$\frac{200}{99} < K < 2.02063$	

Therefore the top predator move towards the gradient of mesopredator only if its population density is large enough compared to that of the mesopredator. The ratio $\frac{e_2}{e_1}$ measures the defensive capacity of the mesopredator in terms of its population size; the larger this ratio, the greater the density of the predator required to advance towards the prey. The parameter values are given by $\alpha = 5$, $a = 2.0$, $b = 5.0$, $c = 0.1$, $d = 2.0$, $\beta = 1.0$, $\gamma = 1.0$, $\mu = 0.05$, $\nu = 0.05$, $d_0 = 0.1$, $d_1 = 1$, $d_2 = 1$. Initial conditions for the spatial distribution of the resource, the meso-predator and top predator are considered as

$$\begin{aligned} u_0(x, y) &= 2 \exp(-10(x^2 + (y - .9)^2))(1 - x^2)^2(1 - y^2)^2; \\ v_0(x, y) &= 2 \exp(-(x + .9)^2 - (y + .9)^2)(1 - x^2)^2(1 - y^2)^2; \\ w_0(x, y) &= 1.5 \end{aligned}$$

for all $x, y \in \Omega$. In contrast with the meso predator and the resource, the top predator is initially uniformly distributed, (see Fig 1).

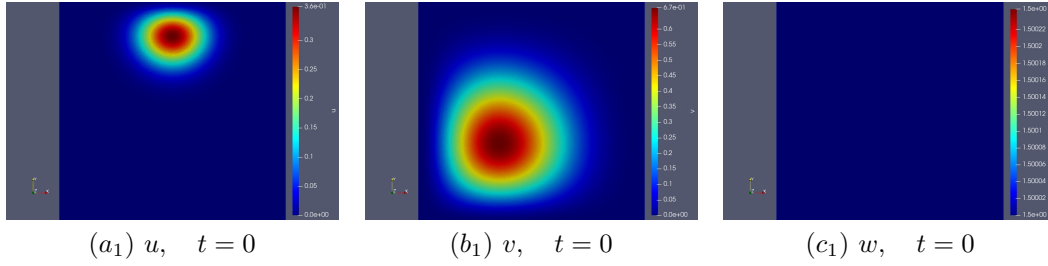


FIGURE 1. *Contour plots* of time evolution of the resource u , meso-predator v and top predator w at different times.

5.1.1. *Defensive capacity and species distribution.* We consider five different defensive capacities of the prey. The suitability of the habitat of the resource is given by

$$\begin{aligned} K(x, y) &= 2 \exp(-5((x + .75)^2 + (y - .75)^2)) + 2 \exp(-5((x - .75)^2 + (y + .75)^2)), \\ &\quad + 2 \exp(-5((x + .75)^2 + (y + .75)^2)) + 2 \exp(-5((x - .75)^2 + (y - .75)^2)). \end{aligned}$$

Notice that the range of K in Ω is contained in the interval $(\frac{2}{99}, \frac{200}{99})$. Therefore, according to Table 1 system 4 without diffusion does not have the coexistence point P_3 and point P_2 is asymptotically stable. Thus, without diffusion the top predator w would become extinct.

First, let $e_1 = 1.0$, $e_2 = 1.0$. In this case, the defensive capacity of the prey is neutral. Top predator move towards mesopredator whenever its density be greater than the one of the mesopredator

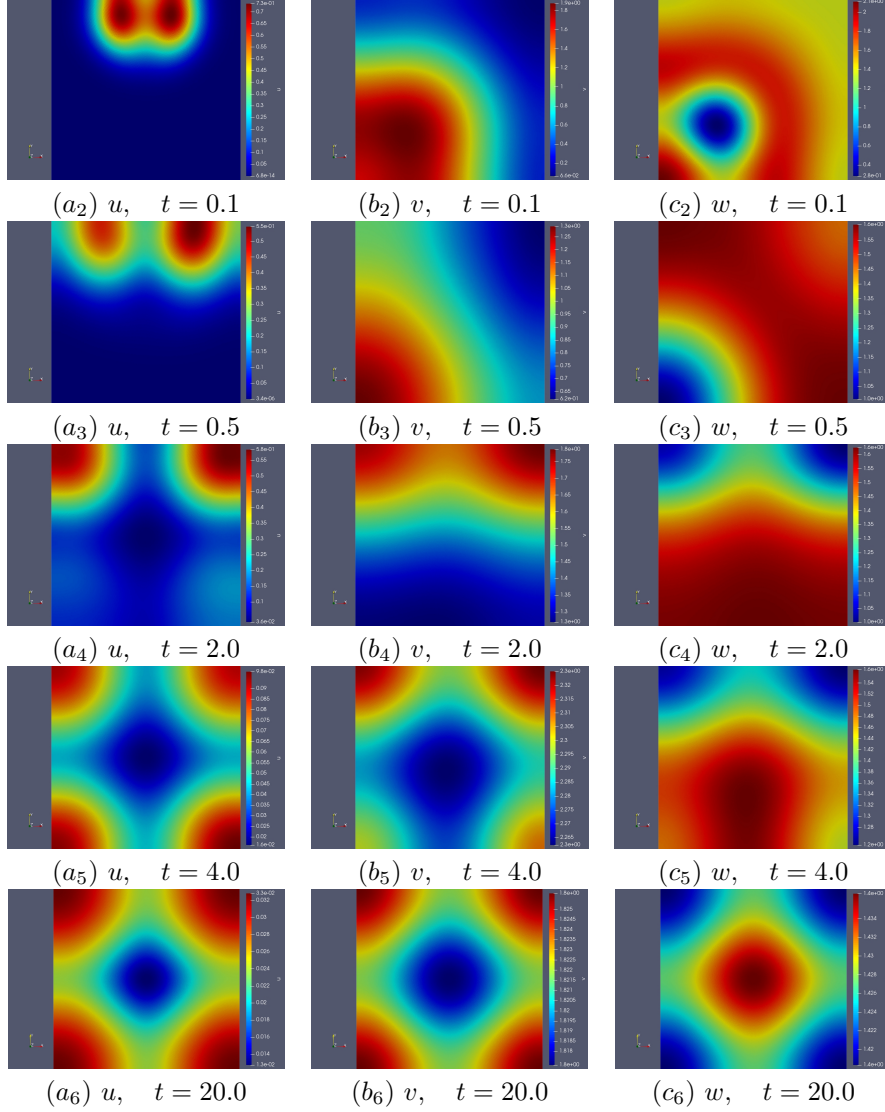


FIGURE 2. Evolution of the spatial distribution of the three species. $e_1 = 1.0, e_2 = 1.0$

Second, let $e_1 = 1.0, e_2 = 0.5$. In this case, the mesopredator defense against of top predator is lesser than the above case. Thus, we observe that predators are closer to the mesopredators than in the first case (see figures 2 and 3).

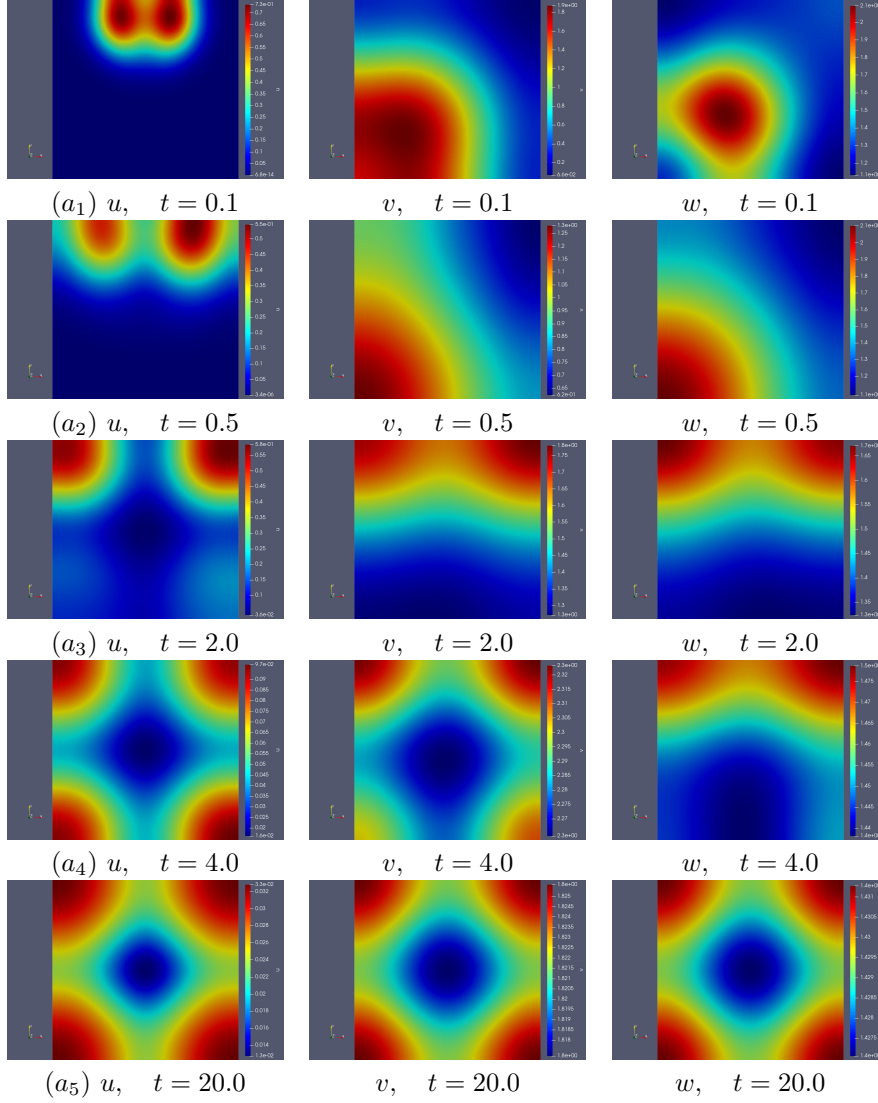


FIGURE 3. Evolution of the spatial distribution of the three species. $e_1 = 1.0, e_2 = 0.5$

Third, let $e_1 = 1.0$, $e_2 = 2.0$. Prey presents a strong defense capacity. Notice that predators tends to move towards the lower density areas of the prey population, (see Figures (2) and (4)).

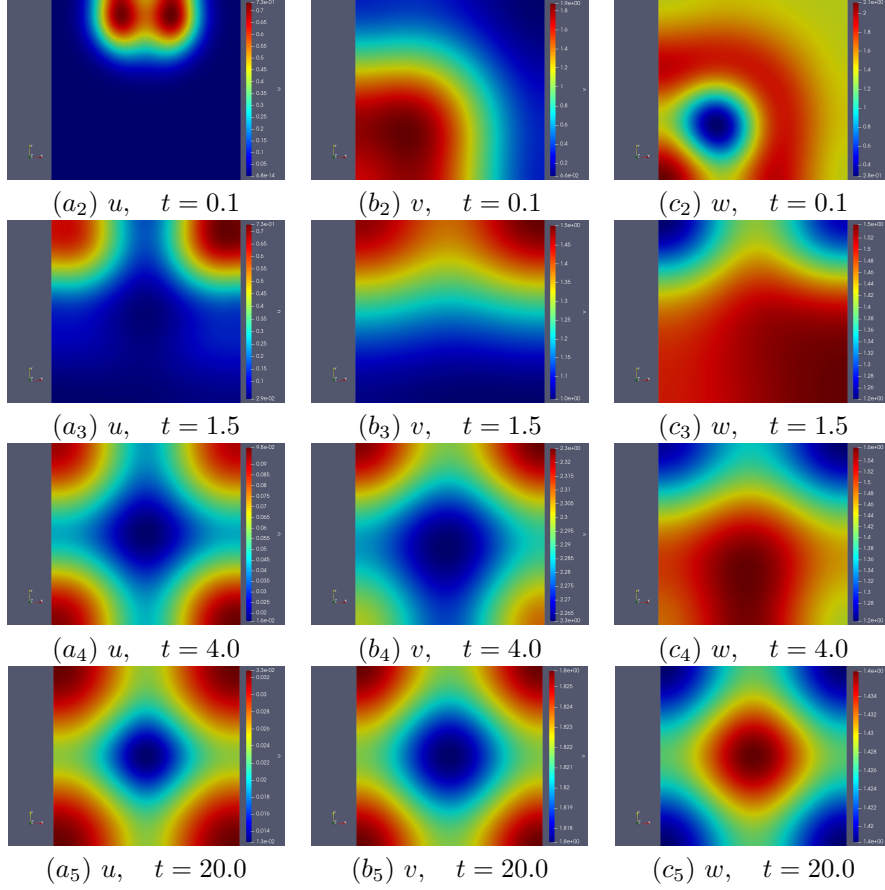


FIGURE 4. Evolution of the spatial distribution of the three species. $e_1 = 1.0, e_2 = 2.0$

Fourth case, let $e_1 = 1.0$, $e_2 = 10.0$. Prey presents still a defense capacity stronger than the previous case.

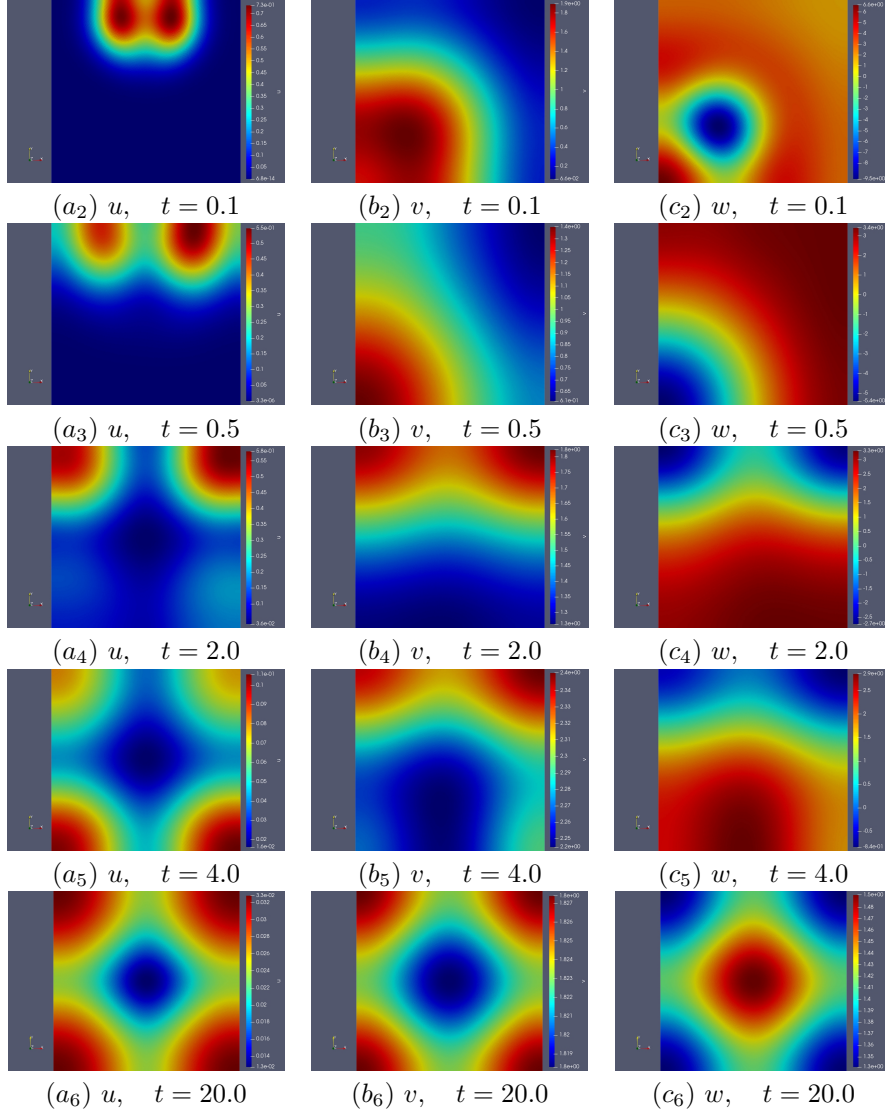


FIGURE 5. Evolution of the spatial distribution of the three species. $e_1 = 1.0, e_2 = 10.0$

Fifth case, Let $e_1 = 10.0$, $e_2 = 1.0$ This is the smallest defensive capacity considered in this section.

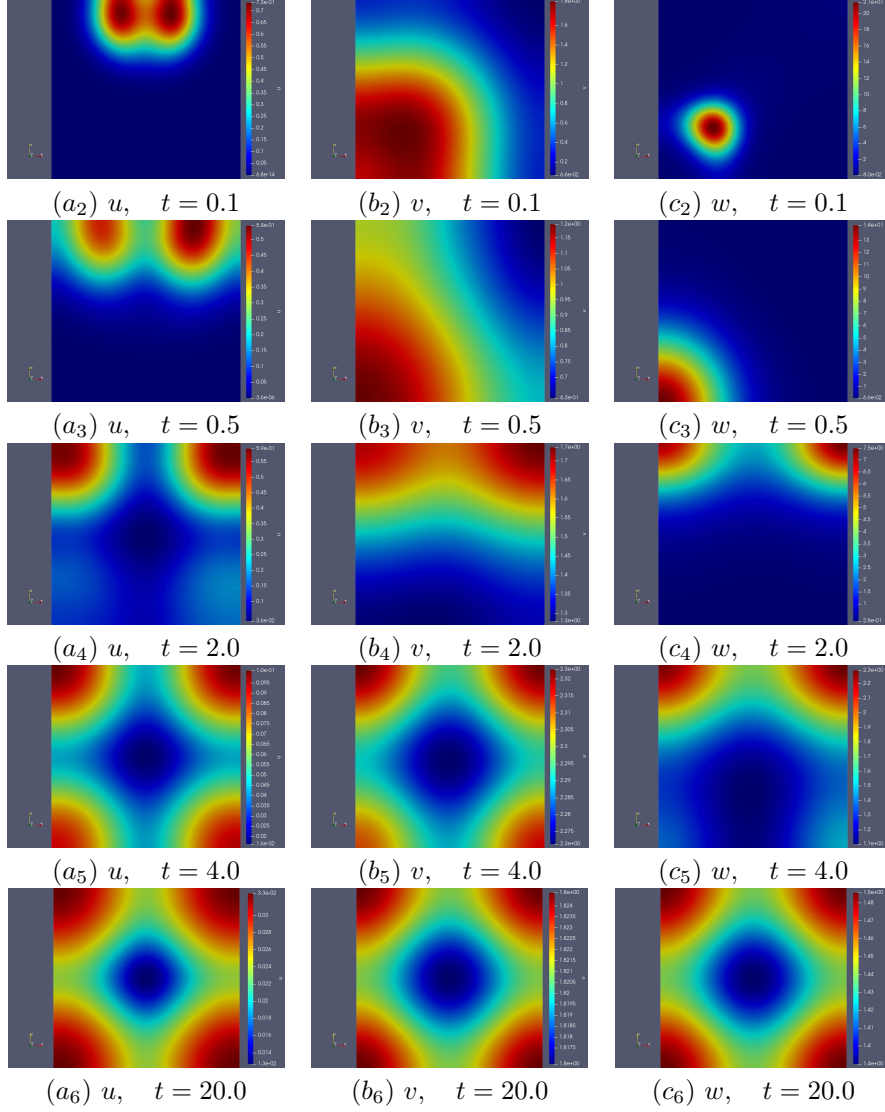


FIGURE 6. Evolution of the spatial distribution of the three species. $e_1 = 10.0$, $e_2 = 1.0$

From the comparison of Figures 3-6, we conclude that defensive capacity has a negligible effect on the prey population, if the predation rate is not large enough. Indeed, the main impact is over the spatial distribution of both the meso predator and the top predator.

5.1.2. *Habitat suitability and species distribution.* To understand how the ecological landscape impact species distribution, we consider two different characterization of the carrying capacity. In either case, the values of parameters of χ_1 are $e_1 = 1.0$, $e_2 = 10.0$, and the initial condition of u is

$$u_0(x, y) = 2 \exp(-10(x^2 + y^2))(1 - x^2)^2(1 - y^2)^2$$

The initial conditions $v_0(x, y)$ and $w_0(x, y)$ are the same as above.

First, we consider a carrying capacity given by

$$\begin{aligned} K(x, y) = & 2 \exp(-5((x + .75)^2 + (y - .75)^2)) + 2 \exp(-5((x - .75)^2 + (y + .75)^2)), \\ & + 2 \exp(-5((x + .75)^2 + (y + .75)^2)) + 2 \exp(-5((x - .75)^2 + (y - .75)^2)). \end{aligned}$$

The highest suitability is reached at four symmetrical points respect to the origin.

In Figure (7) are shown plots of the numerical solutions of u , v and w at different times. Note that as time passes, the resource tends to occupy the most suitable sites. The mesopredator moves towards the sites with the higher resource density and its defensive capacity (e_2/e_1) is large enough to keep the top predator away.

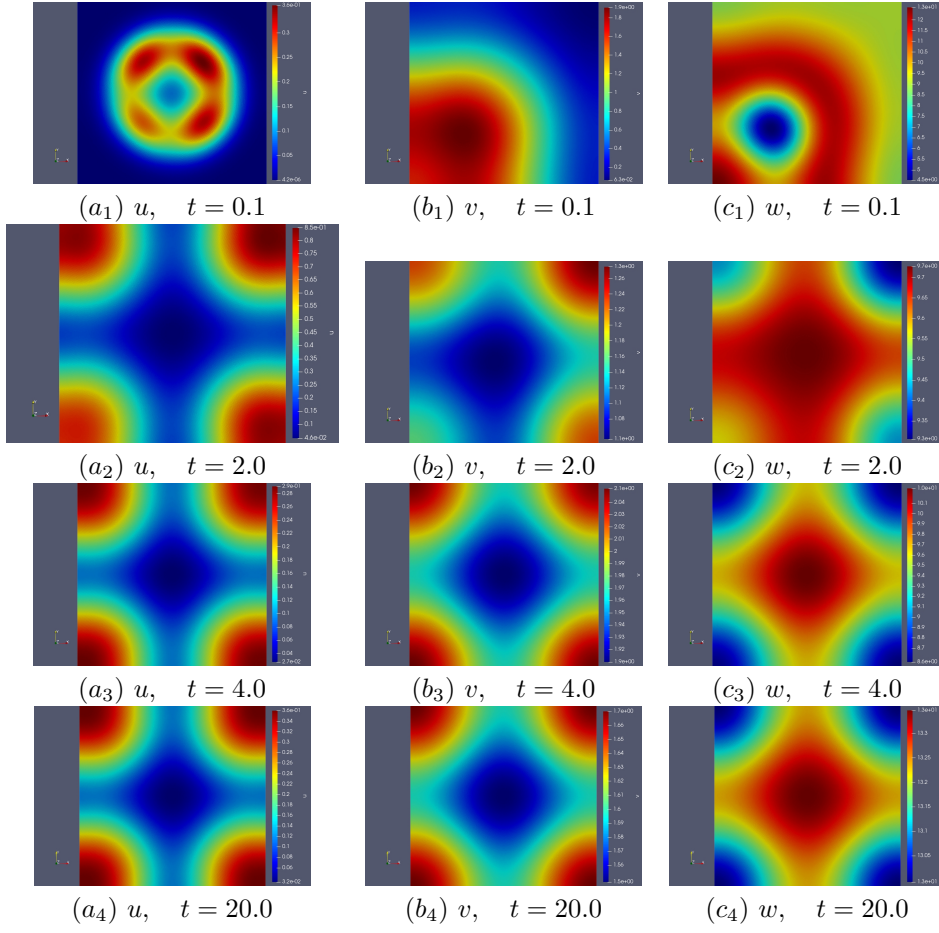


FIGURE 7. Evolution of the spatial distribution of the three species.

In this second case, the habitat of the resource is richer since its suitability is given by

$$K(x, y) = 2 \exp(-5((x + .75)^2 + (y - .75)^2)) + 2 \exp(-5((x - .75)^2 + (y + .75)^2)), \\ + 2 \exp(-5((x + .75)^2 + (y + .75)^2)) + 2 \exp(-5((x - .75)^2 + (y - .75)^2)) \\ + 2 \exp(-5(x^2 + y^2))$$

The highest suitability is reached at four symmetrical points respect to the origin and at the origin. The spatial distribution of the three species is shown in Figure 8.

As in the first case, the mesopredators move towards the sites of higher density of the resource and the top predator is located far enough away from its prey because e_2/e_1 is relatively high. It seems that the richness of the habitat does not induce any change in the distribution patterns. Top predator tends to occupy the areas less densely populated by mesopredators, if e_2/e_1 is high enough.

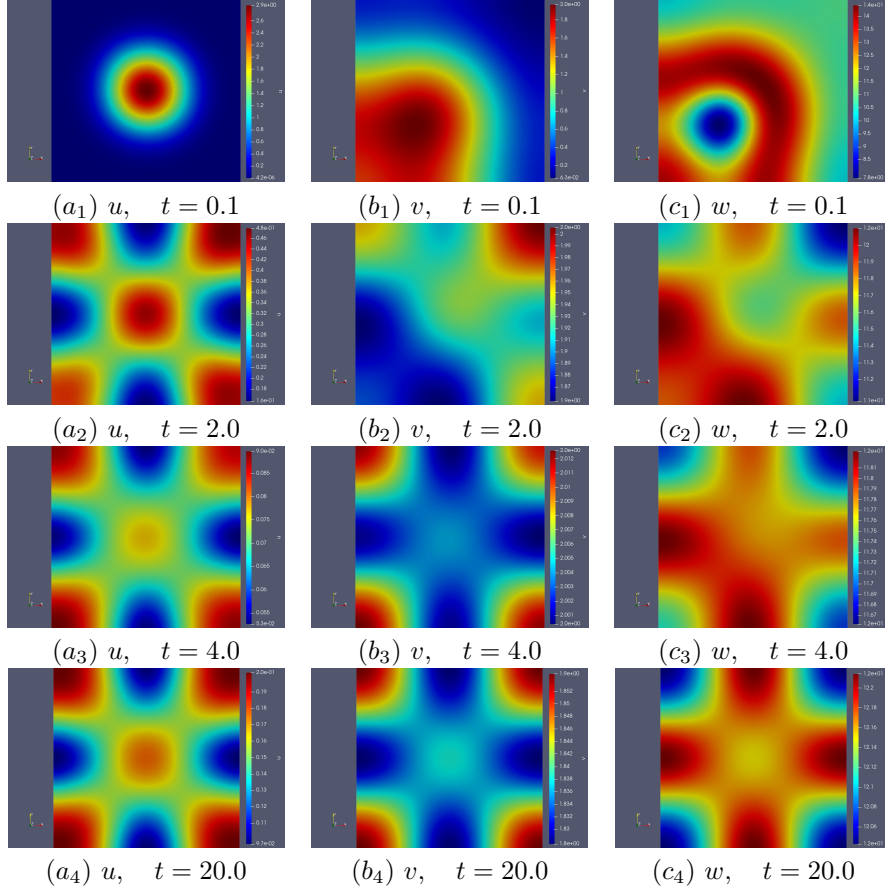


FIGURE 8. Evolution of the spatial distribution of the three species. The suitability of resource habitat is given by (26)

5.2. Resource defense and species distribution. Some species defend themselves by attracting predators from their natural enemies. This is very frequent for instance in plant species, see [21] and the bibliography cited there. In [2] it has been described 24 species of predators which are attracted by volatiles generated by plants damaged by herbivores. In this paper, the authors raise the question about the effectiveness of predator species in controlling specific insect pests. In the following we analyze numerically the impact on the mesopredator distribution of an increasing predation rate of the top predator when this is attracted by the resource species. To analyze the relationship between the distribution of the mesopredator and the predation rate of a top predator that is attracted to the resource, we use Model (2) which is shown below.

$$\begin{aligned}
\frac{\partial u}{\partial t} &= d_0 \Delta u + \alpha u \left(1 - \frac{u}{K(x, y)}\right) - \frac{buv}{u + a}, \\
\frac{\partial v}{\partial t} &= d_1 \Delta v + \gamma \frac{buv}{u + a} - \frac{cvw}{v + d} - \mu v, \\
\frac{\partial w}{\partial t} &= d_2 \Delta w + \beta \frac{cvw}{v + d} - \nu w - \nabla \cdot (\chi_2(u, w) \nabla u).
\end{aligned} \tag{27}$$

The sensitivity function is $\chi_2(u, w) = quw$. Thus, the movement of top predators towards the gradient of u is faster the higher its own density or that of the resource. Initial conditions for the spatial distribution of the resource, the meso-predator and top predator are considered as

$$\begin{aligned}
u_0(x, y) &= 2 \exp(-(x^2 + (y - .9)^2)(1 - x^2)^2(1 - y^2)^2); \\
v_0(x, y) &= 2 \exp(-(x + .9)^2 - (y + .9)^2)(1 - x^2)^2(1 - y^2)^2; \\
w_0(x, y) &= 1.5
\end{aligned}$$

for all $x, y \in \Omega$. The suitability of the habitat of the resource is given by

$$\begin{aligned}
K(x, y) &= 2 \exp(-5((x + .75)^2 + (y - .75)^2)) + 2 \exp(-5((x - .75)^2 + (y + .75)^2)), \\
&\quad + 2 \exp(-5((x + .75)^2 + (y + .75)^2)) + 2 \exp(-5((x - .75)^2 + (y - .75)^2)).
\end{aligned}$$

Let the parameter values be given by $\alpha = 5$, $a = 2.0$, $b = 5.0$, $d = 2.0$, $\beta = 1.0$, $\gamma = 1.0$, $\mu = 0.05$, $\nu = 0.05$, $d_0 = 0.1$, $d_1 = 1$, $d_2 = 1$.

The sensitivity function is $\chi_2(u, w) = quw$. The below simulations are executed for different values of q and c .

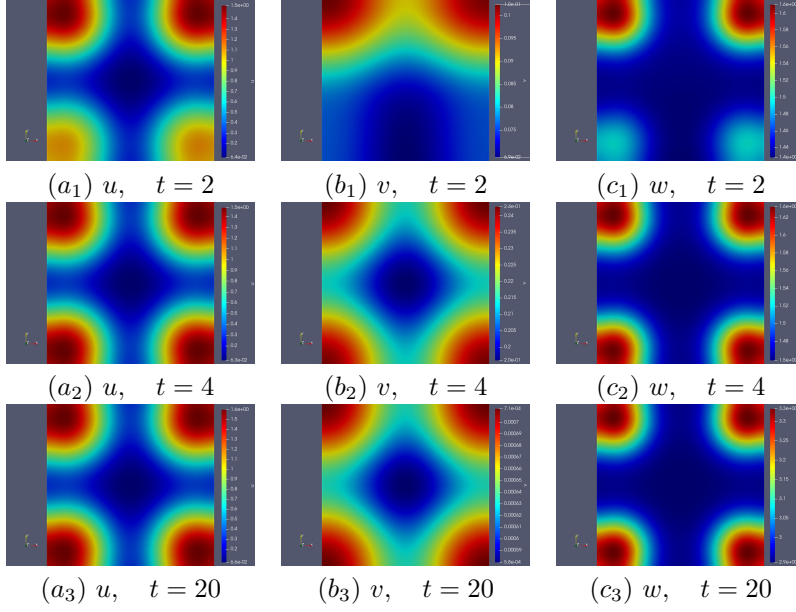


FIGURE 9. *Contour plots* of time evolution of the resource u , mesopredator v and top predator w at different times. $q = 0.1, c = 1.0$

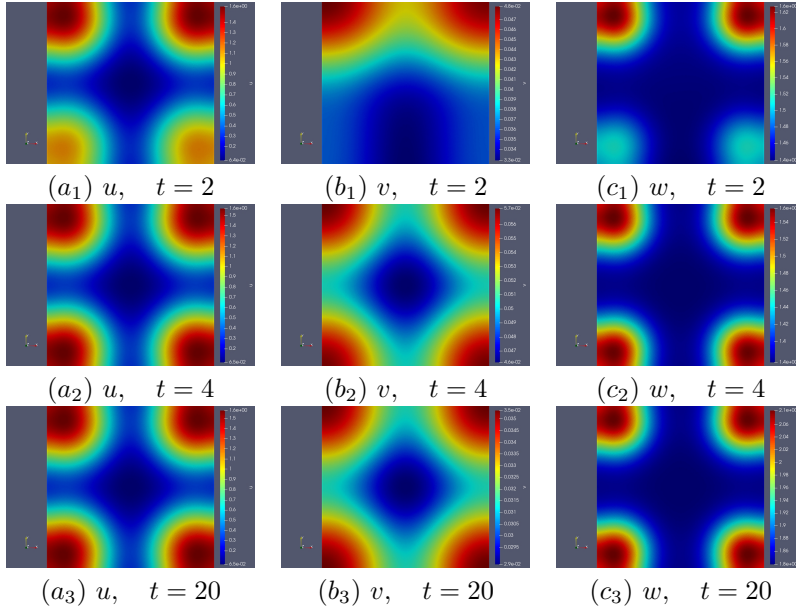


FIGURE 10. *Contour plots* of time evolution of the resource u , mesopredator v and top predator w at different times. $q = 0.1, c = 1.5$

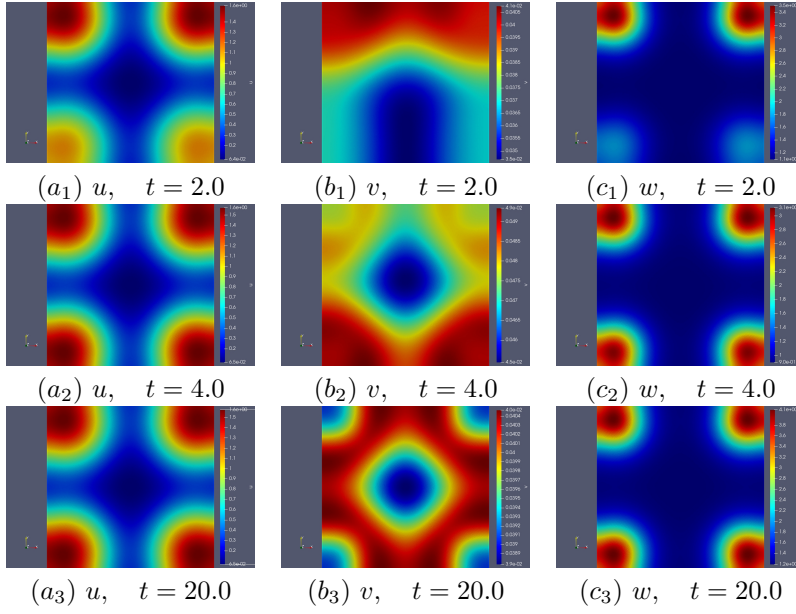


FIGURE 11. *Contour plots* of time evolution of the resource u , mesopredator v and top predator w at different times. $q = 1.0$, $c = 1.5$

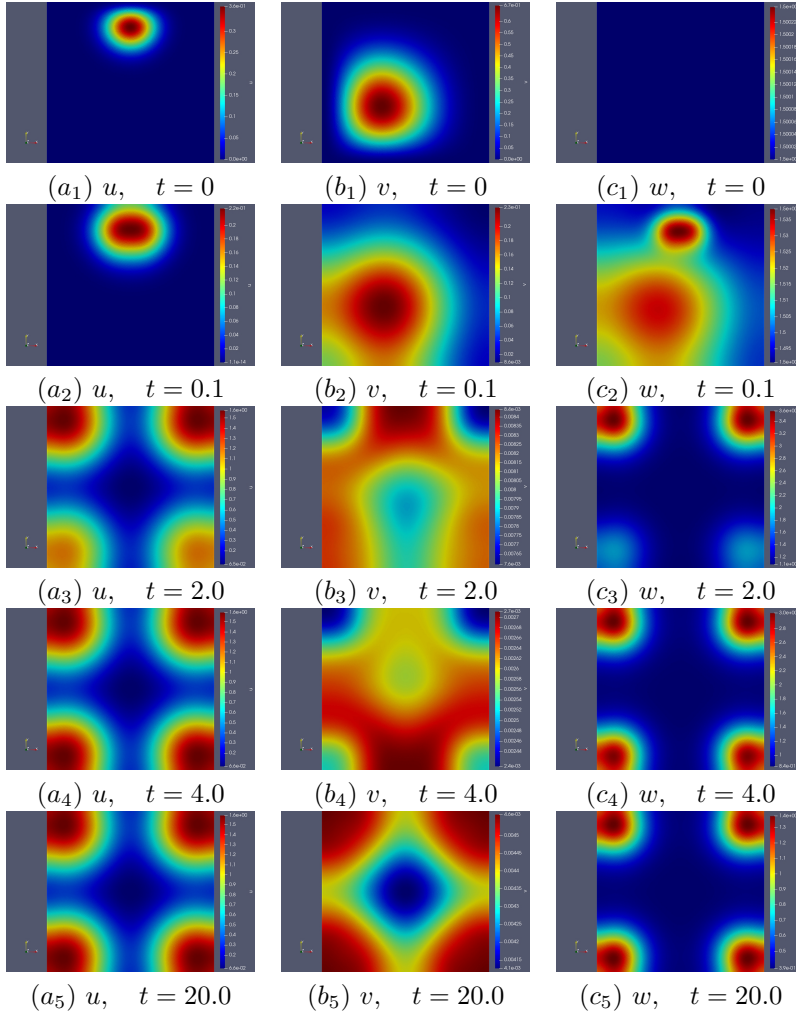


FIGURE 12. *Contour plots* of time evolution of the resource u , mesopredator v and top predator w at different times. $q = 1.0$, $c = 2.5$

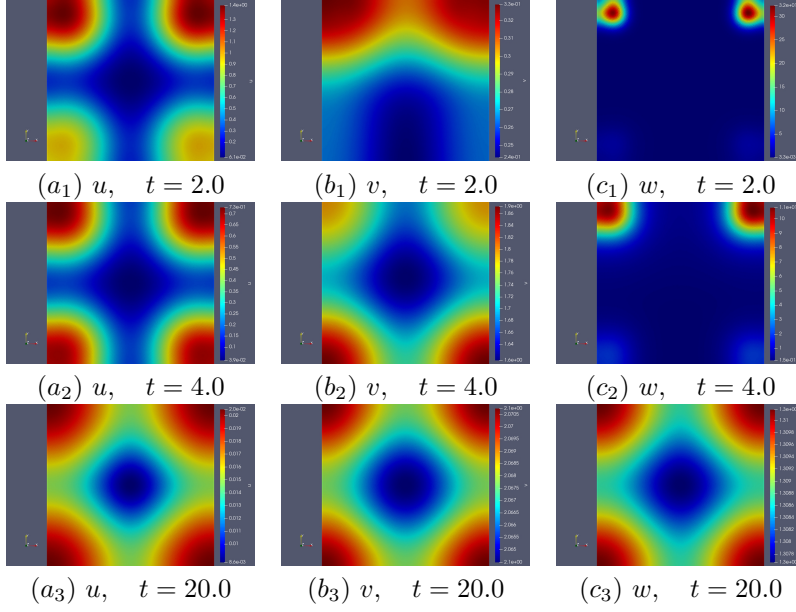


FIGURE 13. *Contour plots* of time evolution of the resource u , mesopredator v and top predator w at different times. $q = 10.0$, $c = .1$

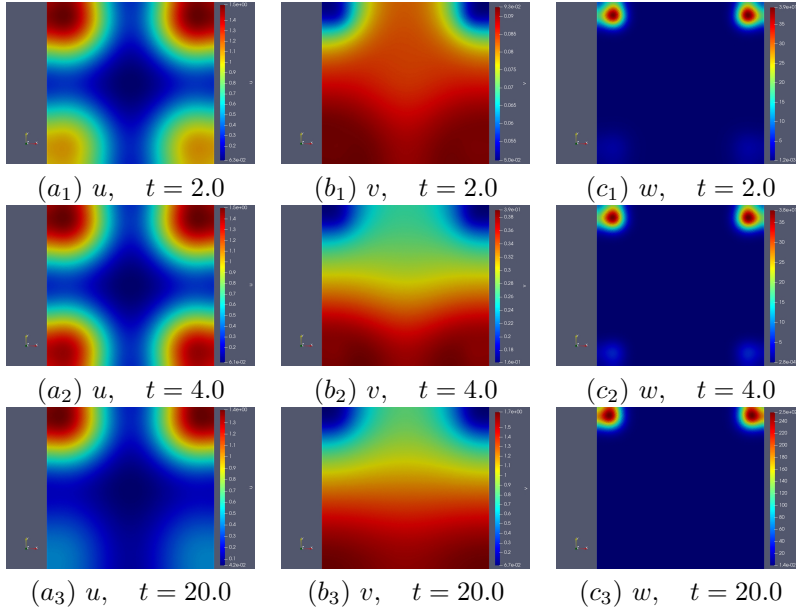


FIGURE 14. *Contour plots* of time evolution of the resource u , mesopredator v and top predator w at different times. $q = 10.0$, $c = 1.0$

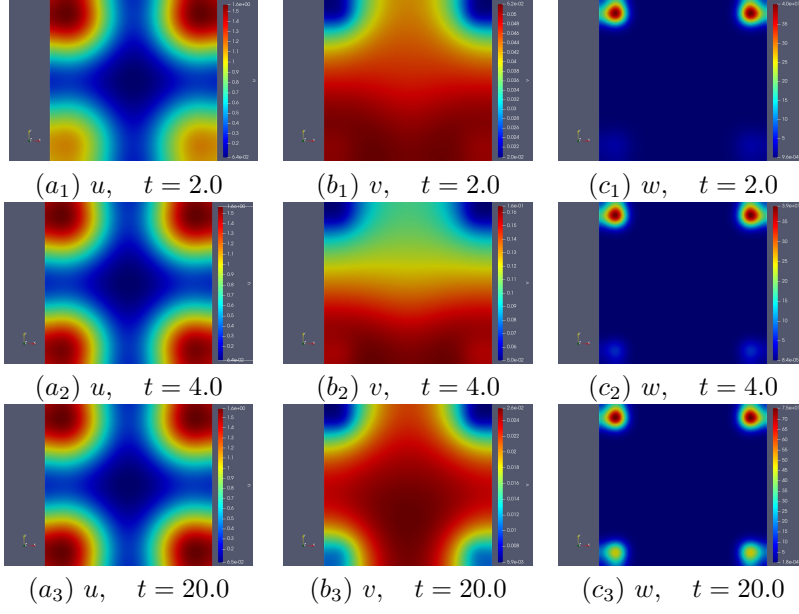


FIGURE 15. *Contour plots* of time evolution of the resource u , mesopredator v and top predator w at different times. $q = 10.0$, $c = 1.5$

It is worth to note that an increment of the predation rate c not necessarily induces an increment on the predator population. In Figure 10 the predation rate is $c=1.5$, and the predator population is lesser than the population showed in Figure 9 where the predation rate is $c = 1.0$. This is due, in part, to the weak attraction of the resource on the individual predators, as this allows predators to remain randomly dispersed throughout space preventing the mesopredator population from reaching a level high enough to support a large population of predators. On the other hand, By comparing Figure 10 with Figure 11 we observe that the main effect on the increment of the attraction parameter q is on the spatial distribution of meso and top predators. For $q = 1.0$ (Figure 11), top predators tend to occupy the places most densely populated by the resource; in contrast, mesopredators occupy the places least densely populated by top predators. However, if the predation rate is large enough, the mesopredator population is depleted and spatial complementarity is lost (see Figure 12). This effect vanishes if the resource's attraction to top predators grows; in fact, for $q = 10$, the separation of top and mesopredators habitats is strengthened for $c = 1$ and all three species reach relatively large populations levels compared to $c = .1$ (See Figure (13-14)). The coexistence of the three species requires a proper balance between the rate of predation and the attraction of predators to the resource population. In Figure 15, we observe very low mesopredator population levels and a sharp concentration of top predators around the areas most populated by mesopredators.

6. Conclusions. With the aim to analyze the role of migration and defensive mechanisms of the prey, in this work two variations of a tritrophic model have been considered. According to Table (1), if the three species remain in the same location (without migration), top predator would become extinct since only the equilibrium point P_2 is stable. In the first case, where a top predator is an active-search hunter it is assumed that as prey density increases, searching intensity decreases (Model (1) with $\chi_1(v, w) = e_1 w - e_2 v$). Numerical simulations show that all three species coexist and both resource and prey tend to be concentrated around sites $(x^*, y^*) \in \Omega$ where resource suitability is greatest; that is, sites (x^*, y^*) where $K(x^*, y^*)$ is the maximum. The spatial distribution of predator depends on the defensive capacity of the prey; for e_2/e_1 low enough, predators and prey have a similar distribution (see Figures (3), (6)). However, if e_2/e_1 reaches a large enough level, the resource and prey populations share the same space, but the predator occupies the locations less populated by prey (see Figures (2), (4), (??)). One second point of interest in this work is how the attraction of enemies of my enemies influences the dynamics of a community. We analyzed this question with Model (2) where the predator moves toward the resource gradient according to the sensitivity function $\chi_2(u, w) = quw$; that is, the higher the population density of the resource or the predator, the greater the tendency of the predator to move towards the resource. In some cases, the attraction activity is caused by volatiles emitted by the resource organisms. The numerical simulations of Model (2) have focused to get some insight about the impact of the attraction that the resource exerted on the predator on the dynamics of the mesopredator-predator interaction. We observe that if the attraction is low enough, the dynamics is mainly determined by the intensity of predation on the mesopredator population, and both mesopredators and predators tend to occupy the sites most populated by the resource. The spatial distribution of the three species shown in Figure 9 ($q = 0.1, c = 1.0$) is very similar

to that shown in Figure 10 ($q = 0.1, c = 1.5$). Notice that the greatest population density of predators and mesopredators are closer to region where the resource is most abundant. However, when the attraction of predators towards the resource increases to a reach a relatively large level, predators follow the spatial distribution of the resource and mesopredators occupy zones where predators are scarce. This is shown in Figure 10, Figure 11 and Figure 15. Hence, our numerical simulations provide evidence that migration favors coexistence and behavioral characteristics, such as a defense mechanism or hunter strategies, can impact the spatial distribution of species. Furthermore, according with the simulations of our two models, we find that the distribution of prey follows a pattern similar to that of the resource, which tends to be distributed near the places of greatest suitability. The cost of a defense mechanism has been considered in [?] where the authors analyze how this cost impact on pattern distribution of predators and preys. The role of predators on the spatial distribution has been studied from an experimental point of view in [17], where preys do not present a defense against predators. They found that was not the patch type but the distribution of predators that most strongly predicted the composition of the prey community. The effect of diffusion on the spatial distribution has been analyzed in [18].

REFERENCES

- [1] Ai S., Du Y., Peng R. *Traveling waves for a generalized Holling–Tanner predator–prey model*. J. Diff. Eq. 2017; **263**(11), 7782–7814.
- [2] Aljbory Z., Chen M. S. *Indirect plant defense against insect herbivores: a review*. Insect Sci. 2018; **25**: 2–23.
- [3] Buonomo B., Gainnino F., Saussure S. and Venturino E. *Effects of limited volatiles release by plants in tritrophic interactions*. MBE. 2019; **16**(5): 3331–3344.
- [4] Ioannou C.C., Krause J. *Searching for prey: the effects of group size and number*. Anim. Behaviour. 2008; **75**(4): 1383–1388.
- [5] Henry D. *Geometrie theory of semilinear parabolic equations*, Lecture Notes in Mathematics 840, Springer, Berlin, 1st ed. 1981. 3rd printing 1993.
- [6] Ross C.T., Winterhalder B. *Sit-and-wait versus hunting: A behavioral ecological model of optimal search model*. J. Theor. Biol. **387**, 76–87, 2015.
- [7] Dumbacher J.P., Pruett-Jones S. *Avian Chemical Defense*. In: Nolan V., Ketterson E.D. (eds) Current Ornithology. Current Ornithology, **13**. Springer, Boston, MA., 1996.
- [8] Denno, R.F., Finke, D.L., and Langelotto, G.A. , *Direct and Indirect Effects of Vegetation Structure and Habitat Complexity on Predator-Prey and Predator-Predator Interactions* in Ecology of predator-prey interactions, Ed. P. Barbosa, I. Castellanos, Oxford Univ. press, pp. 211–239, 2005.
- [9] Eisner, T., Eisner, M., Rossini, C., Iyengar, V. K., Roach, B., Benedikt, E. and Meinwald, J. , *Chemical defense against predation in an insect egg*. PNAS, **97**(4), pp. 1634–1639, 2000.
- [10] Fattorini, D., Notti, A., Nigro, M. and Regoli, F. , *Hyperaccumulation of vanadium in the Antarctic polychaete Perkinsiana littoralis as a natural chemical defense against predation.*, Environ Sci Pollut Res Int. **17**(1), pp. 220–228, 2010.
- [11] Han, R., Dai, B. *Spatiotemporal dynamics and spatial pattern in a diffusive intraguild predation model with delay effect*, Appl. Math. and Comp. **312**, pp. 177–201, 2017.
- [12] Haskell, Evan C., and Jonathan Bell, *Pattern formation in a predator-mediated coexistence model with prey-taxis*, Discrete & Continuous Dynamical Systems-B **22.11** (2017): 0.
- [13] Hecht, F. , *New development in FreeFem++*, Journal of numerical mathematics, **20**, No. 3–4, pp. 251–266, 2012.
- [14] Kessler, A., Baldwin, T. *Defensive function of herbivore-induced plant volatile emissions in Nature*, Science **291**(5511), pp. 2141–2144, 2001.
- [15] Kolmogorov, A., Petrovsky, I. and Piscunov, N. *Etude de l'equation de la diffusion avec croissance de la quantité de matière et son application à une problème biologique*, Bull. Univ. Moscow, Ser. Internat., Sec. A **6**, 1–25, 1937.

- [16] Osorio-Olvera, L., Soberón, J., Falconi, M. *On population abundance and niche structure*, Ecography **42**, 1415–1425, 2019.
- [17] Livingston, G., Fukumori, K., Provett, D.B., Kawacj, M., Takamura, N. and Leibold, M. A. *Predators regulate prey species sorting and spatial distribution in microbial landscapes*, J. Anim.Ecology **86**(3), 501–510, 2017.
- [18] Kumari, N. *Pattern formation in spatially extended tritrophic food chain model systems: Generalist versus specialist top predator*, International Scholarly Research Notices **2013**, 2013.
- [19] Osorio-Olvera, L., Soberón, J., Falconi, M. *On population abundance and niche structure*, Ecography **42**, 1415–1425, 2019.
- [20] Pereira, R.C., Donato, R., Teixeira, V.L. and Cavcanti, D.N. *Chemotaxis and chemical defenses in seaweed susceptibility to herbivory*. Re, Brasil. Biol. **60**(3), pp. 405–414, 2000.
- [21] Price, P.W.; Bouton, C.E.; Gross, P.; McPherson, B.A.; Thompson, J.N.; Weis, A.E. *Interactions among threutrophic levels: Influence of plants on interactions between insect herbivores and natural enemies*. Ann. Rev. Ecol. Syst. **11**, 41–65, 1980,
- [22] Skellam, J.G. *Random Dispersal in Theoretical Populations*. Biometrika **38**(2), pp. 196–218, 1951.
- [23] Song, D., Song, Y. *Stability and Turing patterns in a predator–prey model with hunting cooperation and Allee effect in prey population*, Int. J. Bif. Chaos, **30**(9), 2020.
- [24] Rain, J-B, Fernandez V., Lambert, B., Stocker, R and Seymour, J.R. *The role of microbial motility and chemotaxis in symbiosis*. Nat. Rev. Microbiol **17**, pp. 284–294, 2019.
- [25] Tello, J.I, Wrzosek, D. *Predator–prey model with diffusion and indirect prey-taxis*, Math. Mod. and Meth Appl. Sc. **26**(1), pp. 2129–2162, 2016.
- [26] Matz C, Webb J.S., Schupp P.J., Phang S.Y., Penesyan A., Egan S., Steinberg P. and Kjelleberg S. , *Marine Biofilm Bacteria Evade Eukaryotic Predation by Targeted Chemical Defense*. PLoS ONE **3**(7): e2744, 2008.
- [27] Venturino, E. Petrovskii, S. *Spatiotemporal behavior of a prey–predator system with a group defense for prey*, Ecological Complexity **14**, pp. 37–47, 2013.
- [28] Yang, F., Fu, S. *Global solutions for a tritrophic food chain model with diffusion*. Rocky Mountain J. Math. **38**(5), pp. 1785–1812, 2008.
- [29] D. G. Aronson, *The Role of Diffusion in Mathematical Population Biology: Skellam Revisited*, Mathematics in Biology and Medicine, **57**, pp. 2–6, 1985.
- [30] Douglas, J. and Dupont, T. *Galerkin methods for parabolic equations*, SIAM J. Num. Anal. Vol. 7, No. 4. pp. 575–626 (1970).
- [31] G.A. Polis and Robert D. Holt, *Intraguild Predation: The Dynamics of Complex Trophic Interactions*, Trends Ecol. Evol., **7**, No. 5, pp. 151–154, May 1992.
- [32] V. Thomée, *Galerkin Finite Element Methods for Parabolic Problems*, Springer, Berlin, 2nd Ed. 2006.
- [33] Aljbory, Z., Ming-Shun Chen *Indirect plant defense against insect herbivores: a review* Insect Sci. **25**, 2–23, 2018.
- [34] Wang,K., Wang, Q., Yu., F. *Stationary and time-periodic patterns of two-predator and one-prey systems with prey-taxis*. DCDS- A, **37** (1) : pp. 505–543., 2017.

Appendix A. System (4) has the following equilibrium points

- i) $P_1 (0, 0, 0)$
- ii) $P_2 (K, 0, 0)$
- iii) $P_3 \left(\frac{a\mu}{b\gamma - \mu}, \frac{a\alpha\gamma(b\gamma K - \mu(a+K))}{K(b\gamma - \mu)^2}, 0 \right)$.

Under appropriate conditions, this system posses two equilibrium points $P_4 (u_1, v_1, w_1)$ and $P_5 (u_2, v_2, w_2)$ with positive coordinates given by

$$\begin{aligned}
 u_1 &= \frac{1}{2} \left(-a + K - \sqrt{\frac{c\alpha\beta(a+K)^2 - (4bdK + (a+K)^2\alpha)\nu}{(c\beta - \nu)\alpha}} \right) \\
 v_1 &= \frac{d\nu}{c\beta - \nu} \\
 w_1 &= \frac{(d+v_1)(b\gamma u_1 - (a+u_1)v_1\mu)}{c(a+u_1)} \\
 u_2 &= \frac{1}{2} \left(-a + K + \sqrt{\frac{c\alpha\beta(a+K)^2 - (4bdK + (a+K)^2\alpha)\nu}{(c\beta - \nu)\alpha}} \right)
 \end{aligned}$$

$$v_2 = \frac{d\nu}{c\beta - \nu}$$

$$w_2 = \frac{(d+v_2)(b\gamma u_2 - (a+u_2)v_2\mu)}{c(a+u_2)}.$$

Point P_1 is always unstable; P_2 is locally asymptotically stable if $bK\gamma - a\mu - K\mu < 0$ and unstable if $bK\gamma - a\mu - K\mu > 0$; P_3 is stable if $bK\gamma - a\mu - K\mu > 0$ and $b\gamma a > bK\gamma - a\mu - K\mu$ and unstable if $bK\gamma - a\mu - K\mu > 0$ and $b\gamma a < bK\gamma - a\mu - K\mu$.

If $bK\gamma - a\mu - K\mu < 0$, point $(K, 0, 0)$ is a stable equilibrium point of system 4 (see appendix XX). In the following theorem, we prove that stability of this point is also preserved in the system 1. Let $0 = \mu_1 < \mu_2 < \mu_3 \dots$ be the eigenvalues of the operator $-\Delta$ on Ω with Neumann boundary conditions and let $E(\mu_i)$ be the eigenspace corresponding to μ_i in $C^1(\overline{\Omega})$.

Received xxxx 20xx; revised xxxx 20xx; early access xxxx 20xx.

E-mail address: nestoranaya@hotmail.com

E-mail address: falconi@unam.mx

E-mail address: guilmerg@ciencias.unam.mx